

Communication

# Synergism between B and Nb Improves Fire Resistance in Microalloyed Steels

Pedro Pires Ferreira <sup>1,†</sup>, Felipe Moreno Carvalho <sup>2,†</sup>, Edwan Anderson Ariza-Echeverri <sup>3,4,†</sup>,  
Pedro Meirelles Delfino <sup>3</sup>, Luiz Felipe Bauri <sup>3</sup>, Andrei Marx Ferreira <sup>3</sup>, Ana Paula Braga <sup>2</sup>,  
Luiz Tadeu Fernandes Eleno <sup>1</sup>, Hélio Goldenstein <sup>3</sup> and André Paulo Tschiptschin <sup>3,\*</sup>

<sup>1</sup> Computational Materials Science Group (ComputEEL/MatSci), Escola de Engenharia de Lorena, Universidade de São Paulo, DEMAR, Lorena 12602-810, SP, Brazil

<sup>2</sup> Instituto de Pesquisas Tecnológicas do Estado de São Paulo, São Paulo 05508-901, SP, Brazil

<sup>3</sup> Departamento de Engenharia Metalúrgica e de Materiais, Escola Politécnica, Universidade de São Paulo, São Paulo 01000-000, SP, Brazil

<sup>4</sup> Manufacturing Engineering, Technological University of Pereira, Carrera 27 10-02 Alamos, Pereira 660003, Colombia

\* Correspondence: antship@usp.br

† These authors contributed equally to this work.

**Abstract:** The long exposure of structural components to high temperatures (above 600 °C) negatively changes their mechanical properties, severely compromising the structural capacity of buildings and other structures in which safety is a primary concern. Developing new cheaper fire-resistant steels with better mechanical and thermal performances represents a challenging, cutting-edge materials science and engineering research topic. Alloying elements such as Nb and Mo are generally used to improve the strength at both room and high temperatures due to the formation of precipitates and harder microconstituents. This study shows that adding small amounts of boron in Nb-microalloyed fire-resistant steels may be crucial in maintaining mechanical properties at high temperatures. The widely used 66% yield-strength criteria for fire resistance was achieved at  $\approx 574$  °C for the B-added alloys. In contrast, for those without boron, this value reached  $\approx 460$  °C, representing a remarkable boron-induced mechanical strengthening enhancement. First-principles quantum mechanics calculations demonstrate that boron additions can lower 11.7% of the vacancy formation energy compared to pure ferrite. Furthermore, for Nb-added steels, the reduction in the vacancy formation energy may reach 33.2%, suggesting that the boron-niobium combination could act as an effective pinning-based steel-strengthening agent due to the formation of B-induced higher-density vacancy-related crystalline defects, as well as other well-known steel strengthening mechanisms reported in the literature. Adding boron and niobium may, therefore, be essential in designing better structural alloys.

**Keywords:** microalloyed steels; fire-resistant steels; density functional theory; mechanical properties



**Citation:** Ferreira, P.P.; Carvalho, F.M.; Ariza-Echeverri, E.A.; Delfino, P.M.; Bauri, L.F.; Ferreira, A.M.; Braga, A.P.; Eleno, L.T.F.; Goldenstein, H.; Tschiptschin, A.P. Synergism between B and Nb Improves Fire Resistance in Microalloyed Steels. *Metals* **2023**, *13*, 84. <https://doi.org/10.3390/met13010084>

Academic Editor: Alexander Ivanovich Zaitsev

Received: 28 November 2022

Revised: 23 December 2022

Accepted: 24 December 2022

Published: 29 December 2022



**Copyright:** © 2022 by the authors. Licensee MDPI, Basel, Switzerland. This article is an open access article distributed under the terms and conditions of the Creative Commons Attribution (CC BY) license (<https://creativecommons.org/licenses/by/4.0/>).

## 1. Introduction

Alloying is essential for designing and engineering new materials with optimized properties. For decades, boron (B), for example, has been added to several classes of steels to improve its hardenability [1–6]. It is added to steels at between 10 to 30 ppm to optimize ultimate tensile strength and toughness. When added to steels up to this limit, boron segregates to austenite grain boundaries (AGBs), reducing the grain boundary energy and increasing the hardenability by suppressing the nucleation of allotriomorphic ferrite [7]. Due to boron's high affinity with N and C, higher amounts of boron may induce boron nitrides or boron carbides at the AGBs, acting as nucleation sites for ferrite at high temperatures [5]. Costa et al. [8] studied the effect of boron on quenched and tempered 39MnCrB6-2 steel and showed precipitation of boroncarbides at grain boundaries that embrittled the steel. In addition, steels containing B are less susceptible to distortion and

quenching cracking during heat treatments [9]. Recently, Sharma et al. [6] published a review of the effects of B on heat-treatable steels focusing on some critical aspects. For instance, B can present equilibrium segregation, i.e., redistribution of solute impurities when the temperature increases, causing a decrease in the amount of B solute at the grain boundaries and consequently in the hardenability, or it can cause non-equilibrium segregation by the formation of vacancy-boron that migrates to the grain boundaries. Moreover, B can engage in synergic interaction with some chemical species, such as Mo and Nb, and B-vacancy or complex precipitates, such as  $B_2O_3$ , BN,  $M_{23}(B,C)_6$ , and  $M_7(B,C)_3$ . Therefore, B needs to be protected during steel-making production and heat treatment processes to avoid its precipitation and, consequently, loss of effectiveness in hardenability. One of the most common procedures is to add Ti or Al to protect this effectiveness. In this case, Ti forms the more stable TiN instead of BN, ensuring that boron remains in a solid solution. Ali et al. [10] studied the potential factors that affect the B hardenability in low-carbon alloyed steels, concluding that the formation of coarse precipitates of  $M_{23}(B,C)_6$  in AGBs led to deterioration in toughness and negatively affected the hardenability.

A further essential ingredient for the strengthening of steels is the hindering of dislocation mobility, which is highly desirable to improve the mechanical properties at elevated temperatures, since it mitigates dislocation annihilation with increasing temperature. Recently, Jo et al. [11] proposed that the addition of transition metal solutes, especially the elements Mo and Nb, significantly lowers the vacancy formation energy in Fe-BCC, enabling these lattice defects to be formed easily. Notably, the predicted fraction of vacancy-related defects was confirmed through positron annihilation lifetime spectroscopy by the same authors [11]. These observations led us to search for novel solute combinations through first-principles electronic-structure calculations, aiming to optimize this mechanism. We discovered that small additions of B and Nb to a specific steel composition, surprisingly, led to very significant maintenance of its mechanical properties at fire-level temperatures. Such characteristics can be used with advantage when devising new, cheaper steels with reduced or no molybdenum contents with improved high-temperature properties, ultimately leading to safer buildings and other structures in which safety is a primary concern.

## 2. Materials & Methods

The investigated alloys were produced in an induction vacuum furnace (IDF) and ingoted in a 500 mm × 343 mm × 60 mm mold, producing approximately 80 Kg slabs. The slabs were cut in 260 mm × 50 mm × 19 mm strips, which were soaked at 1200 °C and submitted to thermomechanical controlled rolling (TMCP) to obtain controlled rolled specimens with a fine grain structure of ferrite and carbides. The thermomechanical process was performed with six rolling steps of 76% total reduction thickness, ending above the  $Ac_1$  temperature. Commercial ferroalloys were used to manufacture the studied alloys. The alloys were produced in a pilot plant reproducing the industrial manufacturing processes used in the iron and steel industry. Weight losses and ferro-alloys yields were considered to formulate the materials used in the manufacturing process.

After hot rolling, the plates were air-cooled to room temperature. Isothermal tensile tests were then carried out at room temperature (RT) and 400, 500, 600, 700, and 800 °C to evaluate the yield strength (YS) at 0.2% offset at these temperatures. Mechanical test specimens were taken from the plates in the rolling direction according to ASTM E8/E8M [12] for the RT test and ASTM E21 [13] for the high-temperature (HT) tests. For the isothermal high-temperature tensile tests, the samples were heated to the desired temperature under a heating rate of 10 °C/min, maintained for 15 min for thermal stabilization. Then a strain rate of  $0.00416\text{ s}^{-1}$  was applied until fracture. Finally, after fracture, the samples were air-cooled to room temperature.

The chemical composition of the materials studied is presented in Table 1, one with Fe-C-Mn-Nb-B (with B) and the other with Fe-C-Mn-Nb (without B). The chemical analysis was performed using the wet method employing inductively coupled plasma optical emission spectrometry (ICP-OES). The equipment used to carry out the chemical analysis was

the ICP-OES model by SPECTRO Analytical Instruments GmbH (Kleve, NRW, Germany), which can detect boron as low as 0.59 ppm.

**Table 1.** Chemical composition (in wt.%) of the two ingots used for the experimental investigation.

Alloy	B	C	Nb	Mn	N	Ti
with B	0.0028	0.05	0.10	1.00	0.0029	0.015
without B	0.00	0.05	0.10	1.00	0.0029	0.015

First-principles spin-polarized electronic-structure calculations were performed within the Kohn–Sham scheme [14] of density functional theory (DFT) [15] with scalar-relativistic projector augmented wave pseudopotentials [16] as implemented in Quantum ESPRESSO [17,18]. Exchange and correlation (XC) effects were treated with the generalized gradient approximation (GGA) according to Perdew–Burke–Ernzerhof (PBE) parametrization [19]. We used a kinetic energy cutoff of 70 Ry (1 Ry  $\approx$  13.6 eV) for wave functions and 1120 Ry for the charge density and potential. The Monkhorst–Pack scheme [20] was used for a  $6 \times 6 \times 6$   $k$ -point sampling in the first Brillouin zone. Self-consistent-field (SCF) calculations with a  $10^{-6}$  Ry convergence threshold were carried out using Marzari–Vanderbilt smearing [21] with spread of 0.01 Ry for Brillouin-zone integration. A mixing factor of 0.1 with 12 iterations in a charge density Broyden mixing scheme was used to reach the convergence threshold for self-consistency. All the lattice parameters and internal degrees of freedom were relaxed to guarantee a ground-state convergence of  $10^{-4}$  Ry in total energy,  $10^{-4}$  Ry/ $a_0$  ( $a_0 \approx 0.529$  Å), for forces acting on the nuclei, and  $10^{-6}$  Ry/ $a_0^3$ , for stresses acting on the crystal structure. For further details on the supercell calculations, see, for instance [22].

### 3. Results

According to our results, summarized in Figure 1, it was found that Nb could reduce 14.3% of the vacancy formation energy compared to pure ferrite (2.23 eV), or 10.3% compared to alloys containing Mo (2.13 eV), in remarkable agreement with previous theoretical calculations [11]. However, we found additionally that, when boron is incorporated into the Fe–Nb system, the energy required for a vacancy to be formed becomes 1.49 eV, representing an effective lowering as great as 22% compared to the situation without boron (1.91 eV). These results indicate that the B-induced higher density of vacancy-related defects can act effectively as a trapping barrier to dislocation mobility and, consequently, as a pinning-based steel-strengthening mechanism. The degree of decrease in the vacancy formation energy promoted by the B solid solution in Nb microalloyed ferritic steels represents an enhancement of three orders of magnitude in the amount of vacancy point defects, assuming Arrhenius' law behavior. Therefore, such enhancement is essential to achieve the macroscopic properties of this class of steels. Furthermore, as pointed out by Jo et al. [11], the formation of solute-vacancy pairs and related lattice defects has also been observed in other iron binary alloys with refractory metals [23–26], reinforcing their importance in high-temperature resistance. Our results put a new piece in the puzzle, with B being a potentially central actor in the ongoing fire-resistant steel research endeavor.

However, it is crucial to predominantly find B as a solid solution to reach the above-predicted behavior. Therefore, to probe in which phase boron atoms are predicted to be solubilized, we conducted thermodynamic simulations using ThermoCalc® (TCFE11 database, version 21b, Thermo-Calc Software AB, Solna, Sweden). The simulations were conducted using the base chemical composition given in Table 1, but varying the boron contents as 10, 20, 28 (the *a priori* experimentally desired composition), 30, 40, 50 and 60 ppm. Figure 2 shows the temperature-dependent maximum amounts of boron within the phases for the boron-added alloys. It can be seen that it was possible to solubilize 24.9 ppm of B in the austenite from a global 28 ppm. Running the same simulation for various boron contents, we verified how the solubility of boron in austenite behaved as a

function of the amount of boron added to the material. Notably, the boron solubility limit in austenite was 24.9 ppm regardless of the amount of boron added to the alloy composition.

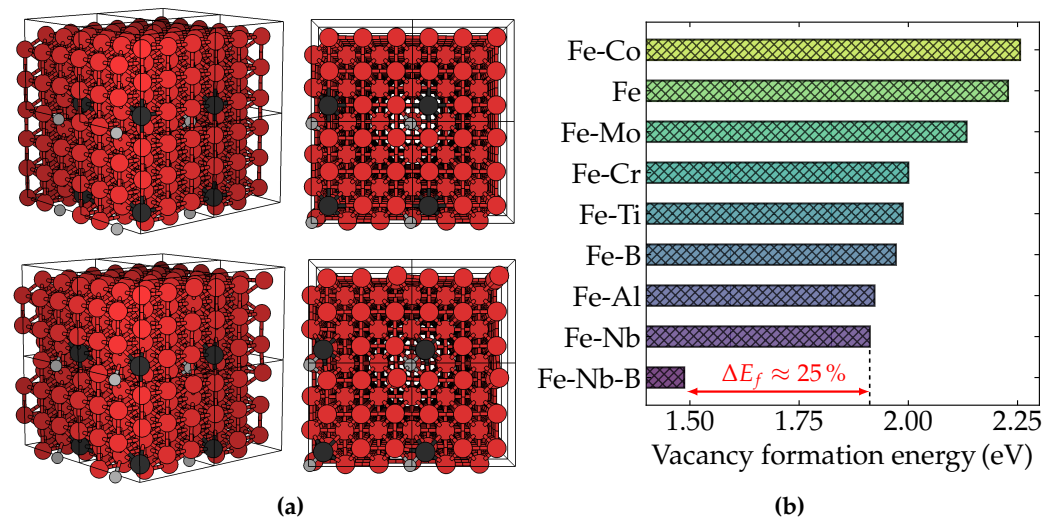


**Figure 1.** First-principles calculations of the Fe-Nb-B structural system. (a) Representation of the  $3 \times 3 \times 3$  supercell used in our calculations. Fe atoms are shown in red, B atoms in light gray, and other solutes in dark gray. The upper panel shows the supercell structures without vacancy, while the lower panel contains the supercell with a vacancy point defect. (b) The DFT-calculated vacancy formation energy of BCC-Fe with several solutes: Fe-Co (2.26 eV), Fe (2.23 eV), Fe-Mo (2.13 eV), Fe-Cr (2.00 eV), Fe-Ti (1.99 eV), Fe-B (1.97 eV), Fe-Al (1.92 eV), Fe-Nb (1.91 eV), Fe-Nb-B (1.49 eV). The percentage difference between the energy required to form a vacancy in Fe-Nb and Fe-Nb-B is almost 25%, as indicated by the red arrow in the figure.

These predictions motivated us to further investigate experimentally the simultaneous effect of B and Nb on improving the mechanical properties at high temperatures. Figure 3a,b show the engineering stress-strain tensile test results of the boron-containing and non-containing alloys performed at 400, 500, 600, 700, and 800 °C. Both alloys showed a reduction in the yield stress associated with increased ductility with increasing temperature. On the other hand, a less severe decay of the yield stress with increasing temperature occurred for the alloy with boron.

In addition to the isothermal high-temperature tensile tests, heating with a constant load applied, also known as accelerated creep testing, was also performed, following the procedure delineated in Walp's investigation [27], which consists of first using a constant load equivalent to a fraction of the yield strength at room temperature and then heating the system at a set rate. While the system heats up, the material yield stress decreases; when a specific imposed stress (constant load) exceeds the material yield stress, the material plastically deforms. As a result, a strain curve can be obtained as a function of temperature. A failure criterion of 1% strain was adopted in the present study, which is consistent with previous reports [28]. A standard creep machine was used to perform the heating, adopting a constant load of 188 MPa (the equivalent of  $\approx 35\%$   $YS_{RT}$  of the alloys) and a heating rate of 5 °C/min. The creep machine was specially manufactured to perform accelerated creep tests in our laboratories, with duly calibrated load cells.

Figure 4a shows the variation in the yield stress with temperature. The literature on fire-resistant structural steels describes several methods to measure the fire resistance of a given material. Based on the ASTM A1077/A1077M standard [29], the literature [27,30] sets a criterion to determine whether structural steel is fire resistant or not, based on the ratio between the yield strength measured at 600 °C ( $YS_{HT}$ ) and the yield strength measured at room temperature ( $YS_{RT}$ ). For a steel to be considered fire-resistant, this ratio ( $YS_{HT}/YS_{RT}$ ) must be greater than two thirds, or 66%. In Figure 4a, the ratio variation as a temperature function for the two alloys studied can be seen.

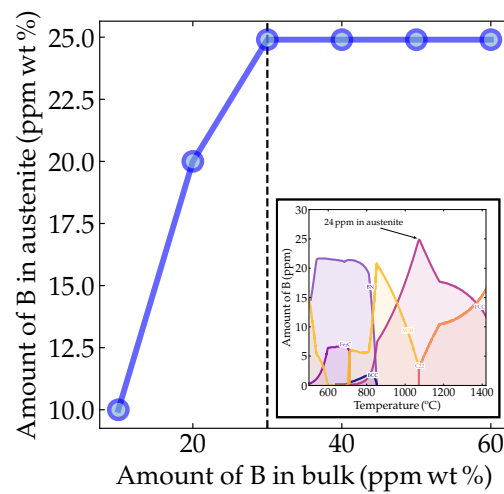


**Figure 2.** Thermodynamic prediction of boron in austenite as a function of the bulk composition. The inset depicts the thermodynamic simulation of the boron content in different microconstituents as a function of temperature, showing a broad peak around 24.9 ppm boron solubility in austenite for the bulk (Nb,B)-microalloyed steel. The calculations were performed using ThermoCalc® with the TCFE11-21b database.

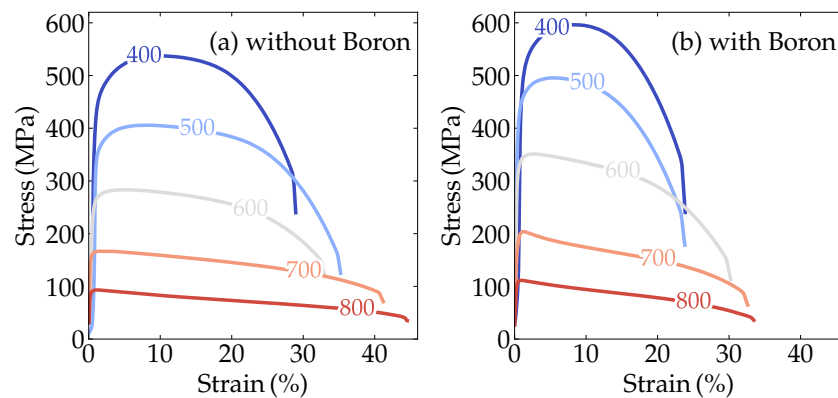


**Figure 3.** Engineering stress-strain curves at high temperatures for the alloy (a) without boron and (b) with added boron.

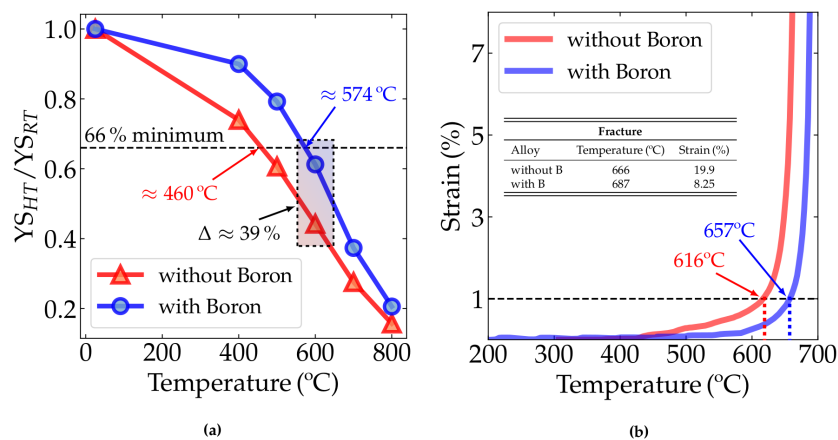


**Figure 4.** (a) Yield strength ratio of the alloys without boron (alloy 1) and with boron-added (alloy 2) at room temperature (RT or 25 °C), 400, 500, 600, 700 and 800 °C; minimum threshold indication of 66% for yield strength ratio at 600 °C with their respective values. (b) Plastic strain with temperature from transient test data—heating rate: 5 °C/min, preload applied: 188 MPa (equivalent to 33% YS<sub>RT</sub> for alloy 1-without B and 36% YS<sub>RT</sub> for alloy 2-with B).

Table 2 shows the room temperature mechanical properties of both alloys. It can be seen in Table 2 that the alloy without B showed a yield strength 8% higher than the alloy with B. However, the boron-added steel maintained a higher yield-strength ratio with increasing temperature. Indeed, in the detached rectangle in Figure 4a, it is clear that  $YS_{HT}/YS_{RT}$  for the boron-added alloy was significantly higher than for those without boron.

**Table 2.** Elongation (E), reduction in area (RA), ultimate tensile strength (UTS), and yield strength (YS) of the studied alloys at room temperature.

Alloy	E (%)	RA (%)	UTS (MPa)	YS (MPa)
with B	19.6	75.8	610	513
without B	20.5	73.2	617	551

The strain vs. temperature data obtained from the constant load test is shown in Figure 4b, where the alloy with boron exhibited better performance at fire-level temperatures. This experiment simulated the fire condition in which a structural beam is subjected to constant load while the temperature increases. In this experiment, the fire resistance may be understood as the temperature required to achieve the 1% strain criterion. Above 450 °C, considering a fixed strain, the alloy with boron shows higher temperature resistance than the alloy without boron. For instance, considering the 1% strain criterion proposed by Speer et al. [28], the B-added alloy resists up to 657 °C, while its counterpart without boron resists up to 616 °C. Therefore, our experiments show that Nb-microalloyed steels containing small amounts of boron offer better fire resistance than those without boron in their composition considering the 1% strain criterion. Considering the fracture point, the alloy with boron will fracture at higher temperatures when compared to the alloy without boron. This may be associated with hardening mechanisms still acting at high temperatures in this material, such as the stabilization of precipitates [11,31–33] and the solid solution of B, enabling the alloy to maintain a considerable part of its yield strength at these temperatures.

Regarding the synergic effect of boron and niobium, Mohrbacher [34] has previously drawn attention to the combined effect of these two alloying elements in Mo-based bainitic and martensitic steels. For instance, the simultaneous addition of B and Nb can retard the static recrystallization of austenite at high temperatures to a more significant degree than the sum of the separate effects due to the formation of Nb-B complexes, consequently reducing the mobility of the grain boundaries [35]. Here, we observed a novel, synergic effect between Nb and B co-alloying in Mo-free steels, in this instance, enhancing the fire resistance properties. The exact detailed structural and macroscopic characterization of these new alloys are topics of ongoing research.

#### 4. Conclusions

To summarize, our investigation demonstrated that simultaneous additions of boron and niobium to fire-resistant steels can lead to significantly better fire-resistance performance under both a constant load test and an isothermal static test, compared to their non-boron counterparts. The 66% YS ratio criterion at RT was achieved at  $\approx 574$  °C for the boron-added Nb-microalloyed steel studied, paving the way to achieving fire-resistant steel compositions with less or even no molybdenum. Furthermore, boron addition in fire-resistant steels significantly improves the stabilization of point defects by lowering the vacancy formation energy (for vacancies close to B atoms), which may play an essential role in reducing dislocation mobility. In this way, we anticipate that our research will motivate further investigations regarding the role of boron and niobium in fire-resistant steel development. We are currently working on a comprehensive study of the characterization and macroscopic mechanisms for a further, more detailed, publication.

**Author Contributions:** Conceptualization, P.P.F., F.M.C., E.A.A.-E., L.T.F.E., H.G. and A.P.T.; methodology, P.P.F., L.T.F.E., H.G. and A.P.T.; software, P.P.F. and F.M.C.; validation, P.P.F., F.M.C. and E.A.A.-E.; formal analysis, P.P.F., F.M.C. and E.A.A.-E.; investigation, P.P.F., F.M.C., P.M.D., L.F.B. and A.M.F.; resources, A.P.B., L.T.F.E., H.G. and A.P.T.; data curation, P.P.F., F.M.C. and E.A.A.-E.; writing—original draft preparation, P.P.F., F.M.C. and E.A.A.-E.; writing—review and editing, P.P.F., F.M.C., E.A.A.-E., L.T.F.E., H.G. and A.P.T.; visualization, P.P.F. and F.M.C.; supervision, A.P.B., L.T.F.E., H.G. and A.P.T.; project administration, A.P.T.; funding acquisition, A.P.B., L.T.F.E., H.G. and A.P.T. All authors have read and agreed to the published version of the manuscript.

**Funding:** This research work has been supported by Companhia Brasileira de Metalurgia e Mineração (CBMM) and Empresa Brasileira de Pesquisa e Inovação Industrial—EMBRAPPII MCE Contract 19.5.02. We also gratefully acknowledge the financial support of the São Paulo Research Foundation (FAPESP) under Grants 2019/05005-7 and 2020/08258-0. This study was financed in part by the Coordenação de Aperfeiçoamento de Pessoal de Nível Superior—Brasil (CAPES)—Finance Code 001 and PROEX—Programa de Excelência Acadêmica n° 0727/2020.

**Data Availability Statement:** The data that support the findings of this study are available from the corresponding author.

**Acknowledgments:** The research was partially carried out using high-performance computing resources made available by the Superintendência de Tecnologia da Informação (STI), Universidade de São Paulo. The authors also acknowledge the National Laboratory for Scientific Computing (LNCC/MCTI, Brazil) for providing HPC resources of the SDumont supercomputer, which have contributed to the research results reported in this manuscript.

**Conflicts of Interest:** The authors declare no conflict of interest. The funders had no role in the design of the study; in the collection, analyses, or interpretation of data; in the writing of the manuscript; or in the decision to publish the results.

## References

1. Lin, H.R.; Cheng, G.H. Hardenability effect of boron on carbon steels. *Mater. Sci. Technol.* **1987**, *3*, 855–859. [[CrossRef](#)]
2. Tsuji, N.; Matsubara, Y.; Sakai, T.; Saito, Y. Proc. of the Int. Conf. on Martensitic Transformations (ICOMAT-92) 767, 1992. *ISIJ Int.* **1997**, *37*, 797–806. [[CrossRef](#)]
3. Gao, Y.; Xue, X.; Yang, H. Influence of Boron on initial austenite grain size and hot deformation behavior of Boron microalloyed steels. *Crystals* **2015**, *5*, 592–607. [[CrossRef](#)]
4. Hu, J.; Du, L.X.; Ma, Y.N.; Sun, G.S.; Xie, H.; Misra, R. Effect of microalloying with molybdenum and boron on the microstructure and mechanical properties of ultra-low-C Ti bearing steel. *Mater. Sci. Eng. A* **2015**, *640*, 259–266. [[CrossRef](#)]
5. Koley, S.; Karani, A.; Chatterjee, S.; Shome, M. Influence of Boron on Austenite to Ferrite Transformation Behavior of Low Carbon Steel Under Continuous Cooling. *J. Mater. Eng. Perform.* **2018**, *27*, 3449–3459. [[CrossRef](#)]
6. Sharma, M.; Ortlepp, I.; Bleck, W. Boron in Heat-Treatable Steels: A Review. *Steel Res. Int.* **2019**, *90*, 1900133. [[CrossRef](#)]
7. Miyamoto, G.; Goto, A.; Takayama, N.; Furuhashi, T. Three-dimensional atom probe analysis of boron segregation at austenite grain boundary in a low carbon steel—Effects of boundary misorientation and quenching temperature. *Scr. Mater.* **2018**, *154*, 168–171. [[CrossRef](#)]
8. Costa, J.P.G.A.; Barboza, M.J.R.; Goldenstein, H.; Nunes, C.A. Borocarbide coarsening and the effect of borocarbide particle size on Charpy V-notch impact properties of medium-carbon boron-containing steel. *Int. J. Mater. Res.* **2020**, *111*, 833–841. [[CrossRef](#)]
9. Ghali, S.N.; El-Faramawy, H.S.; Eissa, M.M. Influence of boron additions on mechanical properties of carbon steel. *JMMCE* **2012**, *11*, 995–999. [[CrossRef](#)]
10. Ali, M.; Nyo, T.; Kajjalainen, A.; Javaheri, V.; Tervo, H.; Hannula, J.; Somani, M.; Kömi, J. Incompatible effects of B and B+ Nb additions and inclusions' characteristics on the microstructures and mechanical properties of low-carbon steels. *Mater. Sci. Eng. A* **2021**, *819*, 141453. [[CrossRef](#)]
11. Jo, H.H.; Shin, C.; Moon, J.; Jang, J.H.; Ha, H.Y.; Park, S.J.; Lee, T.H.; Lee, B.H.; Chung, J.H.; Speer, J.G.; et al. Mechanisms for improving tensile properties at elevated temperature in fire-resistant steel with Mo and Nb. *Mater. Des.* **2020**, *194*, 108882. [[CrossRef](#)]
12. *ASTM E8/E8M-16a*; Standard Test Methods for Tension Testing of Metallic Materials. ASTM International: West Conshohocken, PA, USA, 2016; pp. 1–30. [[CrossRef](#)]
13. *ASTM E21-17*; Standard Test Methods for Elevated Temperature Tension Testing of Metallic Materials. ASTM International: West Conshohocken, PA, USA, 2017; pp. 1–24. [[CrossRef](#)]
14. Kohn, W.; Sham, L.J. Self-consistent equations including exchange and correlation effects. *Phys. Rev.* **1965**, *140*, A1133. [[CrossRef](#)]
15. Hohenberg, P.; Kohn, W. Inhomogeneous electron gas. *Phys. Rev.* **1964**, *136*, B864. [[CrossRef](#)]
16. Dal Corso, A. Pseudopotentials periodic table: From H to Pu. *Comput. Mater. Sci.* **2014**, *95*, 337–350. [[CrossRef](#)]

17. Giannozzi, P.; Baroni, S.; Bonini, N.; Calandra, M.; Car, R.; Cavazzoni, C.; Ceresoli, D.; Chiarotti, G.L.; Cococcioni, M.; Dabo, I.; et al. QUANTUM ESPRESSO: A modular and open-source software project for quantum simulations of materials. *J. Phys. Condens. Matter* **2009**, *21*, 395502. [[CrossRef](#)]
18. Giannozzi, P.; Andreussi, O.; Brumme, T.; Bunau, O.; Nardelli, M.B.; Calandra, M.; Car, R.; Cavazzoni, C.; Ceresoli, D.; Cococcioni, M.; et al. Advanced capabilities for materials modelling with Quantum ESPRESSO. *J. Phys. Condens. Matter* **2017**, *29*, 465901. [[CrossRef](#)]
19. Perdew, J.P.; Burke, K.; Ernzerhof, M. Generalized gradient approximation made simple. *Phys. Rev. Lett.* **1996**, *77*, 3865. [[CrossRef](#)]
20. Monkhorst, H.J.; Pack, J.D. Special points for Brillouin-zone integrations. *Phys. Rev. B* **1976**, *13*, 5188. [[CrossRef](#)]
21. Marzari, N.; Vanderbilt, D.; De Vita, A.; Payne, M.C. Thermal Contraction and Disorder of the Al(110) Surface. *Phys. Rev. Lett.* **1999**, *82*, 3296. [[CrossRef](#)]
22. Dorini, T.T.; de Freitas, B.X.; Ferreira, P.P.; Chaia, N.; Suzuki, P.A.; Joubert, J.M.; Nunes, C.A.; Coelho, G.C.; Eleno, L.T. T2 phase site occupancies in the Cr–Si–B system: A combined synchrotron-XRD/first-principles study. *Scr. Mater.* **2021**, *199*, 113854. [[CrossRef](#)]
23. Wang, X.; Xu, W.; Guo, Z.; Wang, L.; Rong, Y. Carbide characterization in a Nb-microalloyed advanced ultrahigh strength steel after quenching–partitioning–tempering process. *Mater. Sci. Eng. A* **2010**, *527*, 3373–3378. [[CrossRef](#)]
24. Idczak, R.; Konieczny, R.; Chojcan, J. Study of defects in Fe–Re and Fe–Mo alloys by the Mössbauer and positron annihilation spectroscopies. *Solid State Commun.* **2012**, *152*, 1924–1928. [[CrossRef](#)]
25. Idczak, R.; Konieczny, R. Behaviour of vacancies in dilute Fe–Re alloys: A positron annihilation study. *Appl. Phys. A* **2014**, *117*, 1785–1789. [[CrossRef](#)]
26. Idczak, R.; Konieczny, R.; Chojcan, J. A study of defects in iron-based binary alloys by the Mössbauer and positron annihilation spectroscopies. *J. Appl. Phys.* **2014**, *115*, 103513. [[CrossRef](#)]
27. Walp, M. Fire-Resistant Steels for Construction Applications. Ph.D. Thesis, Colorado School of Mines, Golden, CO, USA 2003.
28. Speer, J.G.; Matlock, D.K.; Jansto, S.G. Nb-Microalloyed “Fire-Resistant” Construction Steels: Recent Progress. In Proceedings of the Value-Added Niobium Microalloyed Construction Steels Symposium CBMM and TMS, Singapore, 5–7 November 2012; pp. 133–154.
29. ASTM A1077/A1077M-14; Standard Specification for Structural Steel with Improved Yield Strength at High Temperature for Use in Buildings. ASTM International: West Conshohocken, PA, USA, 2014; pp. 1–3. [[CrossRef](#)]
30. Chijiwa, R.; Tamehiro, H.; Yoshida, Y.; Funato, K.; Uemori, R.; Horii, Y. Development and Practical Application of Fire-Resistant Steel for Buildings. *Nippon Steel Tech. Rep.* **1993**, *58*, 47–55.
31. Wan, R.; Sun, F.; Zhang, L.; Shan, A. Development and study of high-strength low-Mo fire-resistant steel. *Mater. Des.* **2012**, *36*, 227–232. [[CrossRef](#)]
32. Lee, W.; Hong, S.; Park, C.; Kim, K.; Park, S. Influence of Mo on precipitation hardening in hot rolled HSLA steels containing Nb. *Scr. Mater.* **2000**, *43*, 319–324. [[CrossRef](#)]
33. Lee, W.B.; Hong, S.G.; Park, C.G.; Park, S.H. Carbide precipitation and high-temperature strength of hot-rolled high-strength, low-alloy steels containing Nb and Mo. *Metall. Mater. Trans. A* **2002**, *33*, 1689. [[CrossRef](#)]
34. Mohrbacher, H. Synergies of Niobium and Boron Microalloying in Molybdenum Based Bainitic and Martensitic Steels. *Fundam. Appl. Alloy. High Perform. Steels* **2014**, *1*, 83–108.
35. XM, W. Effect of boron addition on structure and properties of low carbon bainitic steels. *ISIJ Int.* **2002**, *42*, S38–S46.

**Disclaimer/Publisher’s Note:** The statements, opinions and data contained in all publications are solely those of the individual author(s) and contributor(s) and not of MDPI and/or the editor(s). MDPI and/or the editor(s) disclaim responsibility for any injury to people or property resulting from any ideas, methods, instructions or products referred to in the content.